

DESIGN OF A WING SECTION AND STRUCTURAL ANALYSIS

**Abstract:** This study presents the process of a wing section design and analysis of structural behavior to evaluate its aerodynamic and structural performance under real flight conditions. The conclusive design of the wing section is determined using the Trefftz plane method. This method provides essential data about critical areas of the structure, and it is used to improve structural and aerodynamic performance.

**Key words:** CFD, wing section, airfoil, NACA, Trefftz plane method, ANSYS

1. INTRODUCTION

This scientific paper intends to study the aerodynamic phenomena that occur on the surface of a wing section during flight conditions by making use of ANSYS. To have an accurate evaluation of the structure, the specific flight conditions of an aircraft (altitude and speed) will serve as input data. Computed information can be used further on as input for finite element analysis.

2. WING STRUCTURAL CHARACTERISTICS

An aircraft’s wing is a complex structural component, essential in achieving the most favourable aerodynamic efficiency. The wing structure must be designed to withstand the forces exerted on its surface during flight without failure. Generally, aluminium is used in designing this type of structure, but recently there have been numerous studies evaluating the characteristics of structures made of composite materials.

A wing section refers to a part of an aircraft wing that includes specific structural components.

The main components of an aircraft wing are the skin, spars, ribs, and stringers. The spars and stringers run perpendicular to the airfoil chord, while the ribs are positioned parallel to it. The skin covers the external surface of the wing and transfers the aerodynamic loads to the internal structure. The main components are illustrated in Figure 1.

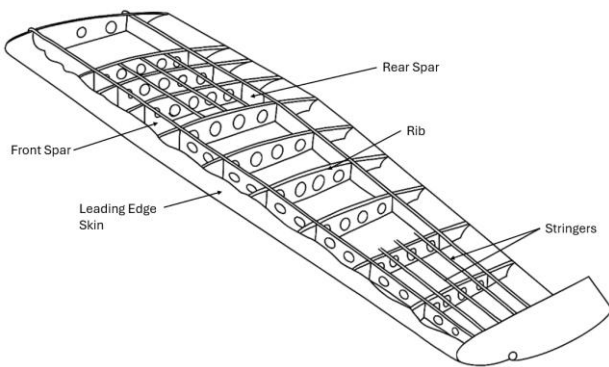


Figure 1 Aircraft wing components [1]

There are several configurations and shapes that can be considered when designing an aircraft. However, the

choice of which type to use varies based on the aircraft mission. It is important to note that the wing design impacts multiple factors such as control at different flight speeds, lift, manoeuvrability, and stability of the aircraft.

Aircraft wings can be classified according to their position on the fuselage as high wing, midwing, and low wing. These configurations are illustrated in Figure 2.

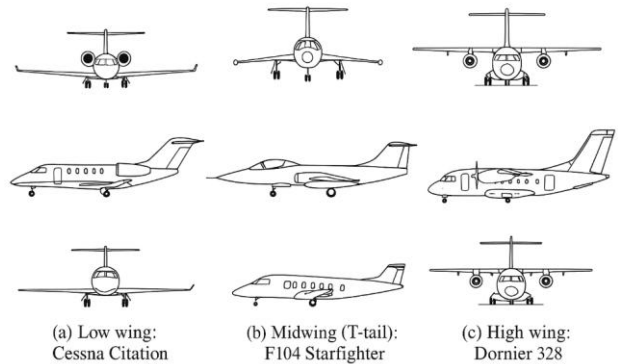


Figure 2 Different wing configurations based on fuselage positioning [2]

Additionally, the wing can be classified according to its shape: elliptic, rectangular, trapezoidal, swept, delta, and ogival. Figure 3 provides an overview of the different wing shapes.

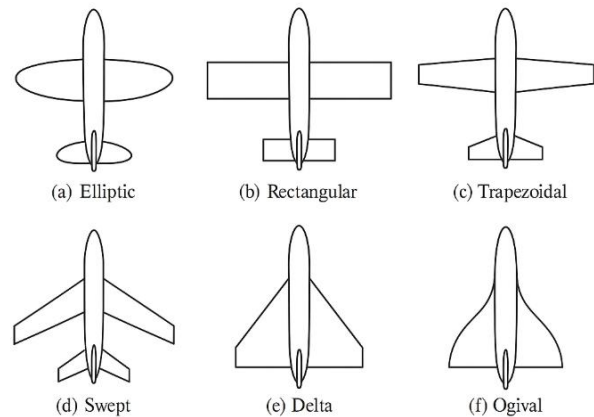


Figure 3 Different wing shapes [3]

The elliptical shape is difficult to manufacture but offers the highest aerodynamic efficiency.

Suitable for military aircraft, the delta wing is primarily used for supersonic flights. An evolved version of the delta wing is the ogival-shaped wing adopted by the famous Concorde.

The majority of commercial aircraft feature swept wings, while the trapezoidal wing is mainly found on charter aircraft.

### 3. FUNDAMENTALS OF AERODYNAMICS

The wing is an aerodynamic structure designed to generate lift while moving through a fluid. This three-dimensional surface is defined by the following elements: span, chord line, and thickness.

An airfoil is the cross-sectional shape of a wing. The key characteristics of an airfoil such as chord line and thickness are shown in Figure 4. Aircraft designed to perform subsonic flight feature airfoils characterized by a round appearance at the leading edge and a sharp appearance at the trailing edge, often with a symmetrical curvature of the upper and lower surfaces.

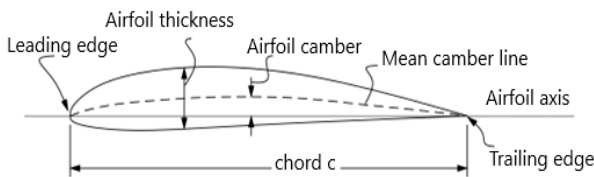


Figure 4 Airfoil characteristics [4]

While an aerodynamic structure is moving through a fluid, it produces a total aerodynamic force. The component of this force that is perpendicular to the wing's direction of motion is referred to as the lift force. The component of the total aerodynamic force that is parallel to the wing's direction of motion is referred to as drag force. A key factor in generating the lift force is the angle of attack, which can be simply defined as angle formed between the relative airflow and the chord line. The forces exerted on an airfoil are illustrated in Figure 5.

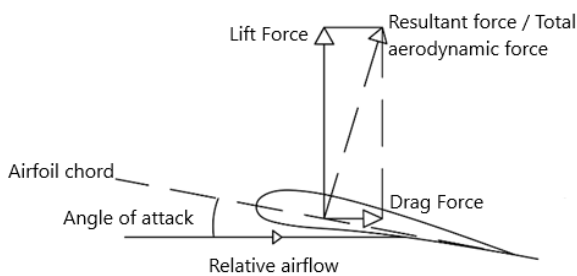


Figure 5 Forces exerted on an airfoil [5]

The aerodynamic efficiency of a wing is expressed by the lift-to-drag ratio. Achieving a high ratio value means that a significantly lower thrust force is required to move the body through a fluid.

Concepts from the field of fluid mechanics are applied in the design and structural analysis of a wing. In theory, the characteristics of fluid flow around a moving body can be determined by solving the Navier-Stokes equations. However, except for the bodies with a simple geometry, these equations are difficult to solve. Therefore, equations with a lower level of complexity are adopted.

To generate lift, the wing must be positioned at a certain angle of attack. Different configurations are presented in Figure 6. When this condition is met, the fluid will be redirected towards the lower surface of the wing. As the wing changes the direction of the fluid by exerting a force on it, the fluid will exert an opposite force on the structure according to the principle of action and reaction. A low-pressure region forms on the upper surface of the wing, while a high-pressure region develops on the lower surface. These pressure differences can be determined directly using specific instruments (wind tunnel) or can be calculated by using Bernoulli's principle.

The lift can be determined using the pressure differences, the different velocities of the fluid on the lower and upper surface of the wing, or the total change in momentum of the deflected air [6]. This discussion is the starting point for selecting the appropriate mathematical approach.

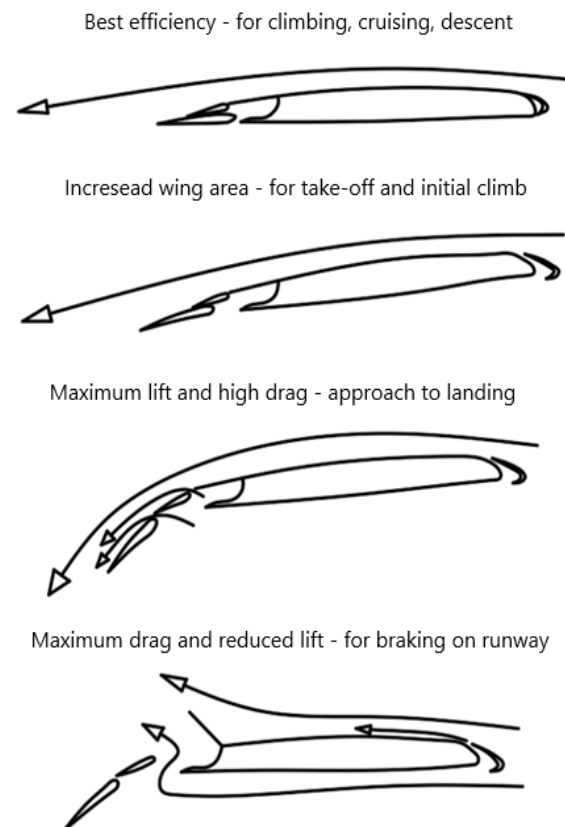


Figure 6 Wing configurations [6]

The flow over a three-dimensional wing is different from the flow over a two-dimensional airfoil section of a wing [7]. Comparing the two scenarios, the main difference observed is an additional component of the fluid acting from the wing tip towards the wing root. Figure 7 illustrates this aerodynamic phenomenon.

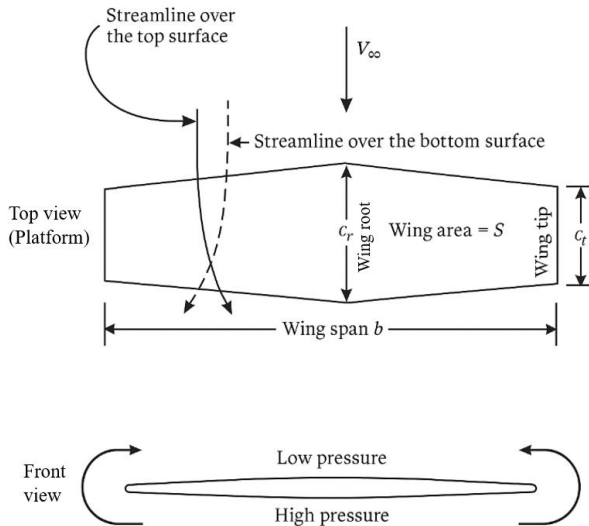


Figure 7 Curvature of streamline in the spanwise direction [7]

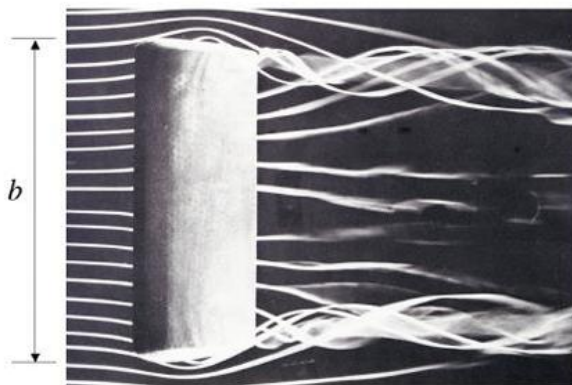


Figure 8 Formation of wing tip vortices on a rectangular wing [7]

As defined earlier, the lift force is generated by the pressure difference between the upper and lower surfaces of the wing. This non-uniform pressure distribution creates lift; however, as a side effect, the airflow tends to curve around the wing tip region, passing from the high-pressure area (lower area of the wing) beneath the wing to the low-pressure area (upper area of the wing). As a result, an additional flow component develops on the upper surface of the wing, directed from the wing tip toward the wing root, which influences the streamlines on both the upper and lower surfaces.

This occurrence has a major importance in aerodynamic studies because the fluid flow at the wing tip creates a circular motion that propagates downstream, resulting in a vortex. The phenomenon is shown in Figure 8, these vortices impact aerodynamic efficiency by increasing the drag force.

#### 4. DESIGN OF THE WING SECTION

Computer-aided design (CAD) has become an indispensable tool today, making it easier to design new products and test their capabilities.

The first step in designing the wing was selecting the NACA 23012 airfoil. The length of the airfoil at the wing root is 1900 mm, while the length of the airfoil at the wing tip is 625 mm [8]. These dimensions were selected to replicate the actual wing geometry of the Cessna 550 Citation II, ensuring more accurate simulation results.

The fundamental concept underlying the design is a multi-spar structure. The wing incorporates two spars with a semi-elliptical cross-section. Conventional components such as ribs and stringers were also integrated into the structural design. The completed design of the wing is illustrated in Figure 9.



Figure 9 Design of the wing structure

Note that the control surfaces (spoiler, flap, and aileron) and the systems contained within the structure (fuel tank, and landing gear) are not considered in the design of the wing, because the final purpose of this study is to analyse the structural behaviour of a wing section. A wing section is a segment of an aircraft wing that is defined by the characteristics of each component. Figure 10 presents the conclusive design of the wing section. Most of the time, for accurate results, the wing is divided into several sections to facilitate structural analysis.

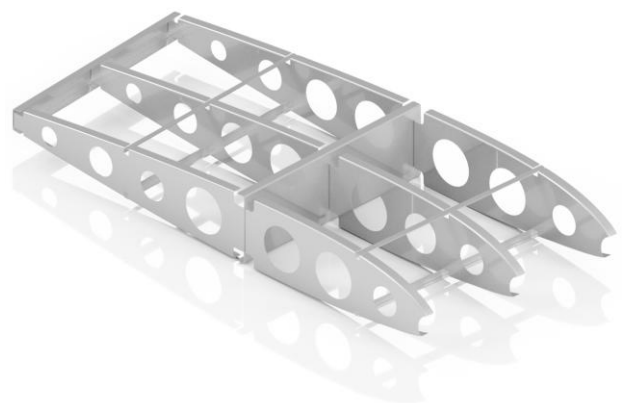


Figure 10 Design of the wing section

### 5. STRUCTURAL CALCULATION APPROACH

There are two methods that can be adopted to calculate the fluid flow over the wing surface: the surface integration method and the Trefftz plane method. This study employs the second method. The Trefftz plane method, also known as the wake integration method, is usually used to calculate the forces and moments exerted on the body under study. Instead of directly evaluating the pressure and forces on the wing surface, the method extracts data from a plane positioned downstream of the wing and perpendicular to the streamlines. Figure 11 illustrates the placement of the Trefftz plane based on the information described above.

The method is related to the integral form of the momentum equation used in fluid mechanics. As a result, the forces acting on a wing can be determined using this method.

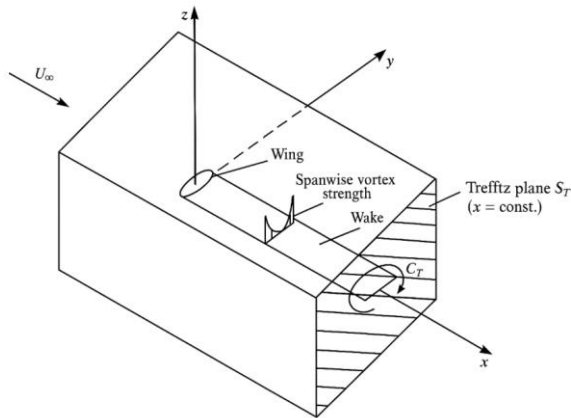


Figure 11 Position of Trefftz plane [7]

Under the assumption of a steady, inviscid flow with no external forces acting on the wing, the momentum equation can be expressed as follows:

$$\int_S \rho q(q \cdot n) dS = F - \int_S p n dS \quad (1)$$

The second term represents the pressure integral. In this domain of interest, a Cartesian coordinate system is applied, oriented parallel to free fluid flow velocity  $U_\infty$  and the velocity vector  $q$ .

$$q = (U_\infty + u, v, w) \quad (2)$$

Calculating the x component of the force (drag), the equation takes the following form:

$$D = - \int_S \rho (U_\infty + u) [(U_\infty + u) dydz + v dx dz + w dx dy] - \int_S p dy dz \quad (3)$$

Next the pressure is determined through the application of Bernoulli's equation:

$$p - p_\infty = \frac{\rho}{2} U_\infty^2 - \frac{\rho}{2} [(U_\infty + u)^2 + v^2 + w^2] = -\rho u U_\infty - \frac{\rho}{2} (u^2 + v^2 + w^2) \quad (4)$$

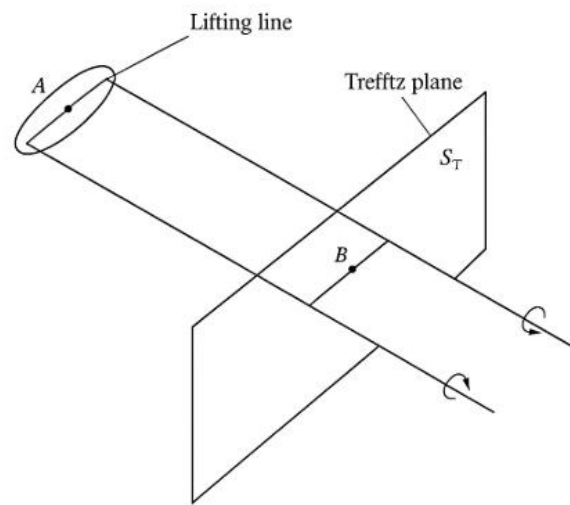


Figure 12 Trefftz plane adopted for the calculation of induced drag [7]

The next step is to insert this equation into the drag equation:

$$D = -\rho \int_S U_\infty (U_\infty + u) dy dz - \rho \int_S (U_\infty + u) (u dy dz + v dx dz + w dx dy) + \rho \int_S u U_\infty dy dz + \frac{\rho}{2} \int_S (u^2 + v^2 + w^2) dy dz \quad (5)$$

By using the continuity equation for perturbations, the terms in the first and third parts of the previous equation simplify. Furthermore, if the domain of interest is sufficiently large, the velocity components disappear everywhere but, on the wake as illustrated in Figure 11.

Velocity components exist only in the y and z directions due to the parallel orientation of the wake relative to the local free stream, as presented in Figure 12, and the ideal flow assumption. The drag is determined by integrating the v and w components on the Trefftz plane.

$$D = \frac{\rho}{2} \int_{S_T} (v^2 + w^2) dydz \quad (6)$$

Equation (6) can be rewritten in terms of vorticity in the following form:

$$D = \frac{\rho}{2} \int_{S_T} \left[ \left( \frac{\partial \phi}{\partial y} \right)^2 + \left( \frac{\partial \phi}{\partial z} \right)^2 \right] dydz \quad (7)$$

## 6. CFD RESULTS AND CONCLUSIONS

### 6.1. SIMULATION RESULTS

After creating the 3D model of the wing section, the CAD file was exported to Ansys. In Design Modeler, the geometry was prepared, and the domains of interest for CFD simulation were defined.

Mesh generation is a crucial step in achieving accurate results. The Ansys Meshing module is used to create a fine mesh on the critical areas.

The next step is to define the computational conditions according to the real flight parameters and the particularities of the Trefftz plane method.

The simulation was iterated 500 times and the results generated are shown in Figures 13-19. Ansys provides these visual representations to illustrate how the fluid flow over the wing section affects parameters such as velocity and pressure.

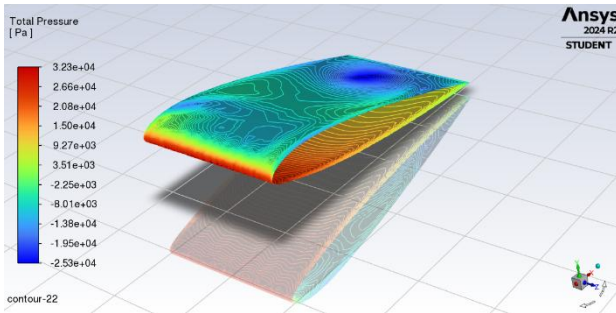


Figure 13 Total pressure

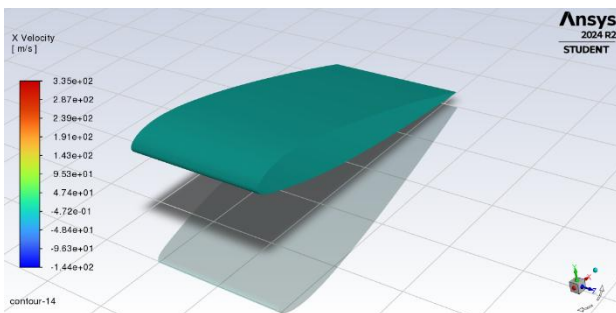


Figure 14 X velocity

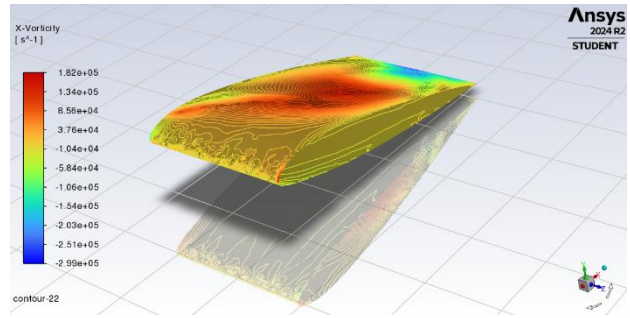


Figure 15 X vorticity

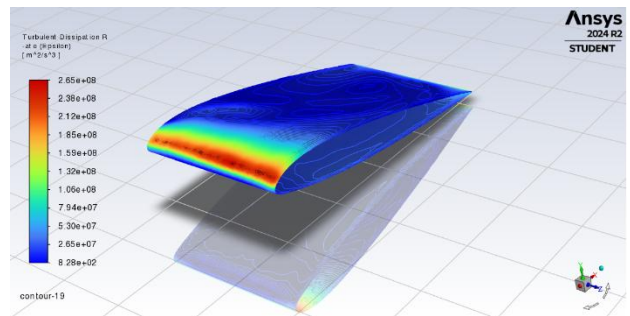


Figure 16 Turbulent dissipation rate

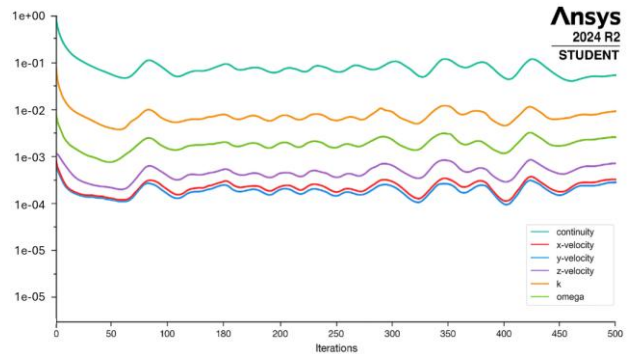


Figure 17 Residuals scaling after 500 iterations

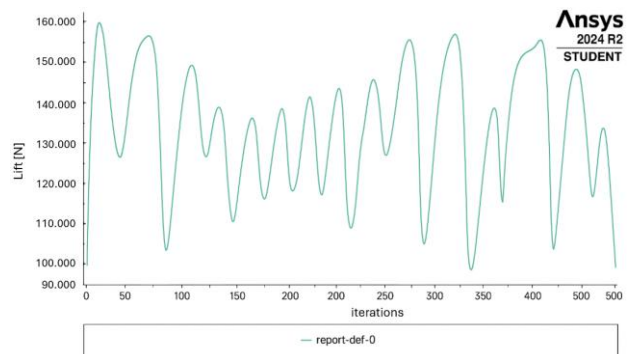
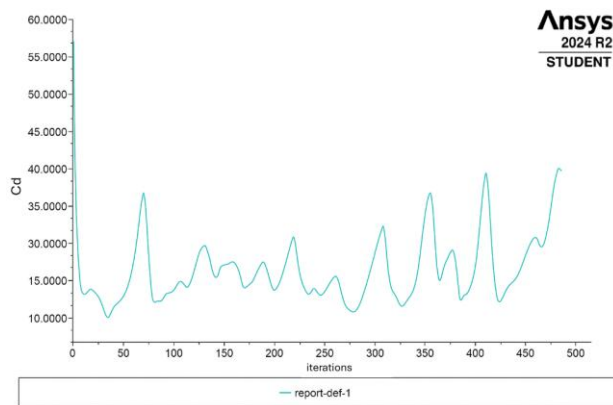


Figure 18 Lift evolution after 500 iterations



**Figure 19** Evolution of drag coefficient after 500 iterations

## 6.2. DISSCUSION

The simulation results shown in Figure 13 reveal a distinct pressure differential between the upper and lower surfaces of the airfoil. The upper surface exhibits lower total pressure values (blue region), indicating a region of accelerated airflow, while the lower surface experiences higher total pressure (red region), corresponding to decelerated flow.

According to Bernoulli's principle, the increase in flow velocity over the upper surface leads to a reduction in pressure, whereas the opposite occurs on the lower surface. This pressure imbalance generates an upward lift force, which is fundamental for sustaining aerodynamic flight.

The velocity field shown in Figure 14 confirms the characteristic aerodynamic behaviour of a lifting airfoil. The upper surface (depicted in red) exhibits higher flow velocities, indicating a region of accelerated airflow as the streamlines follow the curved contour of the airfoil. In contrast, the lower surface (displayed in blue-green tones) presents lower velocities, corresponding to zones of higher static pressure.

According to Bernoulli's principle, the increase in velocity over the upper surface leads to a reduction in static pressure, whereas the decrease in velocity beneath the airfoil results in higher pressure. This velocity gradient between the two surfaces directly contributes to the pressure differential responsible for generating lift, consistent with the total pressure distribution observed in Figure 13.

The vorticity field shown in Figure 15 provides a detailed understanding of the flow rotation and shear layer development around the airfoil. The presence of strong positive vorticity (red zone) over the upper surface suggests a region of intense shear and flow curvature.

Conversely, areas of negative vorticity (blue regions) on the lower surface indicate counter-rotating flow structures or wake formation downstream of the airfoil. These features are indicative of the vortex dynamics that develop due to the velocity differential between the upper and lower surfaces.

The distribution of vorticity confirms the expected aerodynamic behaviour: as the air accelerates over the upper surface, velocity gradients intensify, leading to

localized rotational motion that plays a critical role in defining the lift and drag characteristics of the profile.

The contours in Figure 16 reveal that the highest turbulent dissipation rates occur along the leading edge and the upper surface of the airfoil. These regions are characterized by steep velocity gradients and intense shear, which promote turbulence generation and rapid conversion of turbulent kinetic energy into thermal energy.

As the flow progresses downstream, the dissipation rate decreases, indicating that turbulence becomes less energetic and more diffused. Near the trailing edge, the flow transitions toward a more stable state, consistent with the reduction in vorticity observed in Figure 15.

The distribution pattern confirms that the airfoil experiences turbulent energy losses primarily in regions of strong flow curvature and separation tendency, directly influencing aerodynamic drag and overall efficiency.

The residuals in Figure 17 show a general decreasing trend over the course of the 500 iterations, indicating that the solution is converging toward a steady state. Although small oscillations are visible, particularly in the velocity and turbulence-related quantities, their amplitudes remain stable, suggesting that the solver has reached a numerically steady condition without divergence.

The continuity residual decreases to approximately  $10^{-4}$ , while the velocity and turbulence equations stabilize between  $10^{-3}$  and  $10^{-4}$ , which is acceptable for aerodynamic CFD simulations of this type. This behavior confirms that the computational model achieves an appropriate balance between numerical stability and physical accuracy.

The lift exhibits in Figure 18 periodic oscillations around a mean value of approximately 130–140 N throughout the 500 solver iterations. These fluctuations indicate the presence of unsteady aerodynamic phenomena such as vortex shedding, transient flow separation, or numerical oscillations within the turbulent boundary layer.

Despite these variations, the amplitude of oscillations remains bounded, suggesting that the solution has reached a quasi-steady or statistically steady state, rather than diverging. This behaviour is typical for turbulent external flows over airfoils, where small unsteady structures continuously form and dissipate near the trailing edge, influencing the instantaneous lift coefficient.

The initial portion of the curve (up to around 100 iterations) shows larger oscillations, corresponding to the transient phase of the simulation as the flow field adjusts to the boundary conditions. Beyond approximately iteration 150, the amplitude stabilizes, and the lift force fluctuates around a consistent mean value, confirming numerical convergence of the aerodynamic performance indicators.

The drag coefficient evolution shown in Figure 19, stabilizes after approximately 100 iterations and begins to oscillate around a nearly constant mean value. These oscillations are characteristic of turbulent flow regimes and can be attributed to periodic vortex shedding and

wake fluctuations forming downstream of the airfoil's trailing edge. Such phenomena induce small but continuous variations in the pressure distribution, which directly influence the instantaneous drag force.

This aerodynamic behaviour is consistent with the results obtained for the lift coefficient in Figure 18, where similar oscillatory trends were observed. Together, these findings confirm that the flow around the airfoil exhibits periodic but stable vortex dynamics, which are typical of a turbulent external flow at moderate Reynolds numbers.

### 6.3. CONCLUSIONS

From the analysis of the pressure distribution on the wing section, it can be concluded that there is a zone of high pressure on the lower surface, which indicates the generation of lift force. However, in certain areas exposed to long-term loading, there is a potential risk of structural deformation. On the upper surface of the wing section, a low-pressure area is visible, which reflects the efficiency of the airfoil in generating lift.

Vortex plots indicate losses in aerodynamic efficiency. The areas affected by turbulence are particularly important, as they highlight the regions that require measures to reduce drag force and optimize the overall performance.

The values obtained for the aerodynamic coefficients characterize the overall performance of the wing, and their ratio is essential for evaluating and improving the aerodynamic efficiency.

The lift and drag evolution plots demonstrated oscillatory yet stable behaviour around steady mean values, characteristic of turbulent external flow. Together with the convergence history, these findings validate the robustness of the numerical model and highlight the usefulness of CFD as a predictive tool for optimizing aerodynamic performance and reducing drag in airfoil design.

Based on the results, several improvements can be applied to the model, such as optimizing the aerodynamic

profile to reduce drag. Furthermore, structural performance in critical areas can be enhanced through experimental validations and testing.

### REFERENCES

- [1] Longhurst, G. (2001). *Airframe and Systems: JAA ATPL Theory*, 2nd ed., CLICK2PPSC Ltd.
- [2] Kundu, A. K. (2010). *Aircraft Design*, Cambridge University Press, ISBN: 978-0-521-88516-4, Cambridge, United Kingdom.
- [3] Soler Arrendo, M. (n.d.). *Fundamentals of Aerospace Engineering*, Available at: <https://eng.libretexts.org/> Accessed: 2025-01-03.
- [4] Vawt.ro. (n.d.). *QBlade Tutorial Part 1: Import Airfoil*, Available at: <https://vawt.ro/> Accessed: 2025-01-03.
- [5] Aeroclubul României. (2011). *Principles of Flight*, Aeroclubul României, Bucharest.
- [6] Ergenc, D. (2020). *Aerodynamic Analysis of Aircraft Wing Using Ansys*, DOI: 10.13140/RG.2.2.21551.36003.
- [7] Pannirselvam, M. (2020). *Simulation of Finite Wing Flow and Determination of Induced Drag with Ansys-Fluent*.
- [8] GlobalAir.com. (n.d.). *CITATION II Specifications, Cabin Dimensions, Performance*, Available at: <https://www.globalair.com/> Accessed: 2025-01-07.

### Author(s):

**Eng. Adrian MORARU**, National University of Science and Technology POLITEHNICA Bucharest, Department of Engineering Graphics and Industrial Design, E-mail: [adrian.moraru1107@stud.aero.upb.ro](mailto:adrian.moraru1107@stud.aero.upb.ro)

**Lecturer PhD. Eng. Ioana-Cătălina ENACHE**, National University of Science and Technology POLITEHNICA Bucharest, Department of Engineering Graphics and Industrial Design, E-mail: [catalina.enache@upb.ro](mailto:catalina.enache@upb.ro)